Analytica Chimica Acta 1197 (2022) 339496

Contents lists available at ScienceDirect

Analytica Chimica Acta

journal homepage: www.elsevier.com/locate/aca

Highly reproducible and sensitive electrochemical biosensor for *Chlamydia trachomatis* detection based on duplex-specific nuclease-assisted target-responsive DNA hydrogels and bovine serum albumin carrier platform

Lingjun Cheng [a, 1], Yinghao He [a, 1], Yuanyuan Yang [a], Jiaming Chen [a], Hongzhang He [a], Yinhuan Liu [b, **], Zhenyu Lin [c, *], Guolin Hong [a, ***]

[a] *Department of Laboratory Medicine, Xiamen Key Laboratory of Genetic Testing, The First Affiliated Hospital of Xiamen University, School of Medicine, Xiamen University, Xiamen, 361005, People's Republic of China*

[b] *Department of Laboratory Medicine, Fuzhou Second Hospital, Fuzhou, 350007, People's Republic of China*

[c] *Ministry of Education Key Laboratory for Analytical Science of Food Safety and Biology, Fujian Provincial Key Laboratory of Analysis and Detection for Food Safety, Department of Chemistry, Fuzhou University, Fuzhou, Fujian, 350116, People's Republic of China*

HIGHLIGHTS

- An electrochemical biosensor for *Chlamydia trachomatis* detection has been proposed.
- The ordered loading of capture probes by the BSA vector platform improves the reproducibility.
- Duplex-specific nuclease-assisted DNA hydrogels are used for signal amplification and conversion.
- The biosensor has a low detection limit of 5.8 fM.
- The biosensor has been successfully applied to clinical sample analysis.

GRAPHICAL ABSTRACT

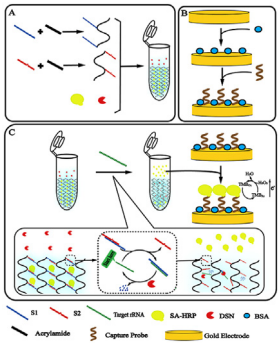

ARTICLE INFO

Article history:
Received 14 December 2021
Received in revised form
9 January 2022
Accepted 11 January 2022
Available online 15 January 2022

Keywords:
Chlamydia trachomatis
16S ribosomal-RNA
Electrochemical biosensor

ABSTRACT

16S ribosomal-RNA (16S rRNA) is often used as an ultrasensitive marker for *Chlamydia trachomatis* (CT) detection because of its species specificity and high copy number in CT. Robust methods for 16S rRNA detection must be developed to realize the early diagnosis of CT infections. In this work, a highly reproducible and sensitive electrochemical biosensor based on duplex-specific nuclease (DSN)-assisted target-responsive DNA hydrogels and bovine serum albumin (BSA) carrier platform for CT detection was developed. Target rRNA can trigger the DNA hydrogel response, which causes it to be repeatedly cleaved by DSN, ultimately leading to the release of a large amount of horseradish peroxidase-labelled streptavidin (SA-HRP) embedded in the hydrogel beforehand. The released SA-HRP was stably captured by the capture probes that were orderly loaded at the gold electrode with the help of a BSA layer. Then, SA-HRP catalyzed the redox reaction of 3,3′,5,5′-tetramethylbenzidine and H_2O_2, producing a current signal that

* Corresponding author. No.2 Xueyuan Road, University Town Fuzhou, Fujian, People's Republic of China.
** Corresponding author. No.47 Shangteng Road, Fuzhou, Fujian, People's Republic of China.
*** Corresponding author. No.55 Zhenhai Road, Xiamen, Fujian, People's Republic of China.
E-mail addresses: yhyh8585@126.com (Y. Liu), zylin@fzu.edu.cn (Z. Lin), xmhgl9899@xmu.edu.cn (G. Hong).
[1] These authors contributed equally to this work.

https://doi.org/10.1016/j.aca.2022.339496

Target-responsive DNA hydrogel
Duplex-specific nuclease
Bovine serum albumin carrier platforms

can be detected. The current signal was proportional to the concentration of CT 16S rRNA from 10 fM to 25 pM with a detection limit of 5.8 fM (S/N = 3). The signal conversion function of the DNA hydrogel avoids the instability of nonhomogeneous nucleic acid hybridization on the gold electrode surface, and combined with optimization by BSA for capture probe modification, this electrochemical biosensor is highly reproducible with a relative standard deviation of 4.3% for the detection of 10 samples of the same concentration. The proposed strategy provides a highly reproducible and sensitive detection method for the extensive screening of CT.

1. Introduction

Chlamydia trachomatis (CT) is one of the most common pathogens of sexually transmitted diseases [1–4]. A significant feature of CT infection is asymptomatic, especially in infected women [5,6]. This circumstance frequently leads to a missed diagnosis, which eventually causes severe diseases such as pelvic inflammatory disease and tubal infertility [7–9]. Therefore, extensive screening is needed to facilitate the identification of asymptomatic infections. Classical microscopic examination is not suitable for screening because it is inefficient and insensitive, and has been gradually replaced by more sensitive nucleic acid detection [10]. Nucleic acid detection is a highly specific detection method using deoxyribonucleic acid (DNA) or ribonucleic acid (RNA) as pathogenic markers. The commonly used methods are based on polymerase chain reaction (PCR), and much effort is still required to develop robust methods for CT-related nucleic acid detection.

Electrochemical detection techniques are widely used in pathogenic nucleic acid detection because their high sensitivity, simple equipment, ease of miniaturization and low cost [11,12]. For example, Songyi Baek reported an electrochemical DNA biosensor based on a metal ion-mediated molecular beacon (MB) probe for CT sensitive detection [13]. Sang Mo Lee's group developed an electrochemical strategy to sensitively detect CT related DNA based on peroxidase mimicking DNAzyme [14]. These studies indicated that high sensitivity can be reached for CT related nucleic acid detection based on electrochemical detection. However, a large proportion of reported electrochemical nucleic acid sensors are based on thiol-derivatized single-stranded DNA probes self-assembling on a gold surface via Au-S chemistry and then passivated with alkanethiol to fill the empty space, thereby capturing the target nucleic acid [15,16]. The reproducibility of the detection signal is affected because of the random nature of probe self-assembly on gold electrodes and the instability of the subsequent nonhomogeneous nucleic acid hybridization process on gold electrodes [17–19]. Many groups have devoted great efforts to improving reproducibility [20,21]. For instance, Ye et al. developed three-dimensional (3D) DNA tetrahedron-structured probes that could provide mechanical rigidity and structural stability to achieve stable electrochemical detection of microRNA-21 [21]. However, they are complex in construction and remains randomly assembled on the surface of gold electrodes. To avoid electrode modification steps and nonhomogeneous nucleic acid hybridization processes, He et al. proposed a homogeneous electrochemical detection strategy based on the electrostatic repulsion between DNA and the surface of an indium tin oxide electrode [22]. Although this strategy can achieve good results, the possible matrix interference limits the specificity and wide application in bioassays.

DNA hydrogels, as a stable aqueous soft material, can provide a homogeneous environment that stably responds to the stimulus of the target by releasing the encapsulated signal molecules [23]. The ability of DNA hydrogels to convert target quantities into more readily detectable signal molecular quantities has driven the development of many efficient and stable biosensors [24–29]. For instance, Liu et al. reported an electrochemical biosensing platform based on hybrid DNA hydrogels [30]. DNA hydrogels can respond to microRNA-21, leading to the release of electrochemical signalling indicators, which realize the rapid detection of microRNA-21.

16S ribosomal-RNA (16S rRNA) has approximately 10,000-fold the copy number of genomic DNA in CT and varies between species, so it is used as a more sensitive nucleic acid target for CT [31,32]. The bovine serum albumin (BSA) carrier platform can effectively improve the reproducibility of electrochemical signals by preferentially modifying BSA onto gold electrode surface to facilitate the ordered assembly of subsequent probes. It enables highly reproducible detection of *Cryptococcus neoformans* and human papillomavirus [33,34]. The procedures of this technique are simple, but its use is still in the early stages.

In this work, a highly reproducible electrochemical biosensor was designed for CT detection using the 16S rRNA fragment as an ultrasensitive target. Duplex-specific nuclease (DSN) can highly selectively cleave DNA strands in perfectly matched DNA double-strands (dsDNA) and DNA-RNA hybrid duplexes [35–37]. In combination with the cycle amplification of the DSN, target-responsive DNA hydrogels are applied to identify the target, amplify the signal and convert the amount of target into the amount of signal molecule being released. The porous BSA layer improves the positional distribution and spatial orientation of the capture probe modified on the gold electrode, allowing it to stably capture the released signal molecule. With the above strategy, the low efficiency and instability of nonhomogeneous nucleic acid hybridization on gold surfaces are avoided, as well as the randomness of electroactive material capture and the influence of other substances on the electrical signal, enabling highly reproducible and sensitive CT electrochemical detection.

2. Experimental section

2.1. Materials

All oligonucleotides were obtained from Shanghai Sangon Biotechnology Co., Ltd., (Shanghai, China). The sequences ware as follows:

DNA strand 1 (S1): Acrydite-AAAAACTTAGG**GGCCGAC**T**AACCC**.
DNA strand 2 (S2): Acrydite-AAAA**GGGTTAC**T**CGGCC**.
Capture probe: SHC6-TTTTTTTTTTTTTTTTTTT-Biotion.
CT rRNA: GGGUUAGUCGGCCCUAAGU.
MG rRNA: UAGGUCGCAAGCGUUAUCCG.
NG rRNA: CUAACUACGUGCCAGCAGCC.
UU rRNA: GCGUAAAACGAGCGCAGGCG.

Unless otherwise stated, all chemicals were purchased from commercial suppliers and used without further purification. The buffer 10 × NE Buffer 2 (1 × NE Buffer 2 containing 50 mM NaCl, 10 mM Tris-HCl, 10 mM $MgCl_2$, pH 7.9) was obtained from New

England BioLabs (Beijing, China). Duplex-specific nuclease was supplied by Evrogen Co., Ltd., (Moscow, Russia). H_2SO_4, $K_4Fe(CN)_6$, $K_3Fe(CN)_6$, acrylamide, ammonium persulfate (APS), N, N, N′, N′-tetramethylethylenediamine (TEMED), horseradish peroxidase-labelled streptavidin (SA-HRP), phosphate buffered saline buffer (PBS buffer containing NaCl 136.9 mM; KCl 2.7 mM; Na_2HPO_4 8.1 mM; KH_2PO_4 1.8 mM), bovine serum albumin (BSA) and ribonuclease-free H_2O were sourced from Shanghai Sangon Biotechnology Co., Ltd., (Shanghai, China). The enhanced k-blue 3,3′,5,5′-tetramethylbenzidine substrate (TMB containing H_2O_2) was purchased from Neogen Co., Ltd., (Lansing, America). The CT nucleic acid detection kit was obtained from Rendu Biotechnology Co., Ltd., (Shanghai, China). All solutions were prepared with ribonuclease-free H_2O.

2.2. Equipment

Electrochemical measurements were carried out on a CHI660E electrochemical workstation (Shanghai Chenhua Instruments Co., Ltd., China) with a traditional three-electrode configuration comprised of a gold working electrode (3 mm in diameter), an Ag/AgCl reference electrode and a platinum wire auxiliary electrode.

2.3. Preparation of DNA hydrogel

S1 or S2 was mixed with 4% acrylamide solution and dried under vacuum for 15 min to remove oxygen. Then 0.14% of freshly prepared APS and 0.14% of TEMED were added, and dried at 37 °C for 60 min to form polymer strand 1 (P-S1) or polymer strand 2 (P-S2). Then, P-S1, P-S2, NE Buffer 2 and SA-HRP were mixed at a ratio of 3 μL: 3 μL: 1 μL: 1 μL, heated at 65 °C for 10 min with good shaking and slowly dropped to room temperature to form DNA hydrogel. Next, 20 μL of target rRNA at various concentrations containing 1 μL of 10 mU DSN was added to the DNA hydrogel. Then, the mixture was incubated at 35 °C for 60 min, and the supernatant was removed and dropped onto the surface of the prepared gold electrode.

2.4. Gold electrode modification and electrochemical detection

The gold electrode was first polished with alumina slurry, and ultrasonically cleaned with ultrapure water. Then, the gold electrode was scanned to activate in a 0.5 M H_2SO_4 solution. Eventually, the gold electrode was flushed with ultrapure water and dried with nitrogen. Afterwards, 10 μL of PBS buffer containing 5 mg/mL BSA was dropped onto the newly cleaned surface of the gold electrode and incubated at room temperature for 15 min. Then, 7 μL of 5 μM thiol-modified and biotin-modified capture probe was dropped onto the activated gold electrode and placed at 37 °C for 2 h to bind to the gold electrode by the Au-S bond.

After dropping the supernatant onto the surface of the prepared gold electrode for 30 min, current versus time curves (i-t curves) were obtained by amperometric detection using an electrochemical workstation. Amperometric detection was carried out on the TMB and H_2O_2 substrates. The initial potential was 0 V; the sample interval was 0.1 s; and the run time was 100 s. Three measurements were taken for each result and averaged as shown in the error bars.

2.5. Polyacrylamide gel electrophoresis analysis, electrochemical impedance spectroscopy and cyclic voltammetry curve analysis

A 20% polyacrylamide gel was used for electrophoresis to verify the cross-linking of the DNA hydrogel, and explore the feasibility of a specific response of the DNA hydrogel for the target rRNA. The buffer solution was 0.5 × TBE, the working voltage was 80 V, and electrophoresis was performed at room temperature for 360 min.

Electrochemical impedance spectroscopy (EIS) was used to characterize the modification process of the gold electrode. The modified electrode was placed in a solution containing 0.1 M KCl and 10 mM $K_3[Fe(CN)_6]/K_4[Fe(CN)_6]$ to observe the variations in electron transfer resistance (Ret) after each modification step.

Cyclic voltammograms were used to characterize the adsorption behaviour of proteins on the electrode surface. After dripping 10 μL of PBS buffer containing 5 mg/mL BSA on the bare gold electrode, let sit for different times, then rinse and detect it in a solution of 100 mM $K_3Fe(CN)_6$ and 0.1 M KCl, in the potential range of −0.4 to −0.7 V with CV scan at a rate of 100 mV/s.

2.6. Clinical sample analysis

To verify the performance of this strategy in detecting CT 16S rRNA in clinical samples, urine or cervical examination samples from patients at the First Affiliated Hospital of Xiamen University were collected, tested and analysed. First, these clinical samples were tested by a CT nucleic acid detection kit and the results were obtained. Furthermore, our strategy was used to test these samples. Finally, different concentrations of CT 16S rRNA sequences were added to the sample nucleic acid extracts and assayed as described above. This research project complied with the “Declaration of Helsinki”, and was approved by the local ethics committee of the School of Medicine, Xiamen University. In addition, written informed consent was obtained from all participants.

3. Results and discussion

3.1. The principle of the proposed biosensor for CT 16S rRNA detection

As shown in Scheme 1, acrydite-DNA strand 1 (S1) and acrydite-DNA strand 2 (S2) were copolymerized with acrylamide monomers to obtain the corresponding DNA-polyacrylamide complexes, polymer strands 1 (P-S1) and polymer strands 2 (P-S2), respectively. After mixing, P-S1 and P-S2 hybridized to form a 16S rRNA-responsive hydrogel, and a large amount of SA-HRP was encapsulated in the hydrogel. In the DNA hydrogel, the S1-S2 double-stranded (S1-S2 dsDNA) formed by the hybridization of S1 and S2 has a set of mismatched base pairs, so it cannot be cleaved by DSN without the help of the target rRNA. When the target rRNA is present, the target sequence displaces S1 from the S1-S2 dsDNA by a strand displacement reaction, forming an S1-rRNA hybrid duplex. The S1-rRNA hybrid duplex was then specifically recognized by DSN, which mediated the digestion of S1 in the S1-rRNA hybrid duplex. After digestion, the target rRNA was released and recovered for another round of hybridization and digestion. Thus, in this practical strategy, target rRNA was recycled by DSN, leading to the collapse of the hydrogel and the release of a large amount of SA-HRP, which achieved signal amplification and conversion. On the other hand, a BSA carrier platform was designed to capture the released SA-HRP by first modifying BSA on the surface of a gold electrode to form a porous layer with regular interstices and then fixing thiol-modified and biotin-modified capture probes in these interstices. The assembled capture probes were evenly distributed on the electrode surface, reducing the randomness of the probe assembly and stabilizing the capture of SA-HRP by the affinity-biotin system. Finally, the captured SA-HRP catalyzed the redox reaction between H_2O_2 and TMB, producing a significant electrochemical signal. The detected electrochemical signal was positively correlated with the target concentration, thus allowing the development of an electrochemical biosensor for the highly reproducible quantitative detection of CT.

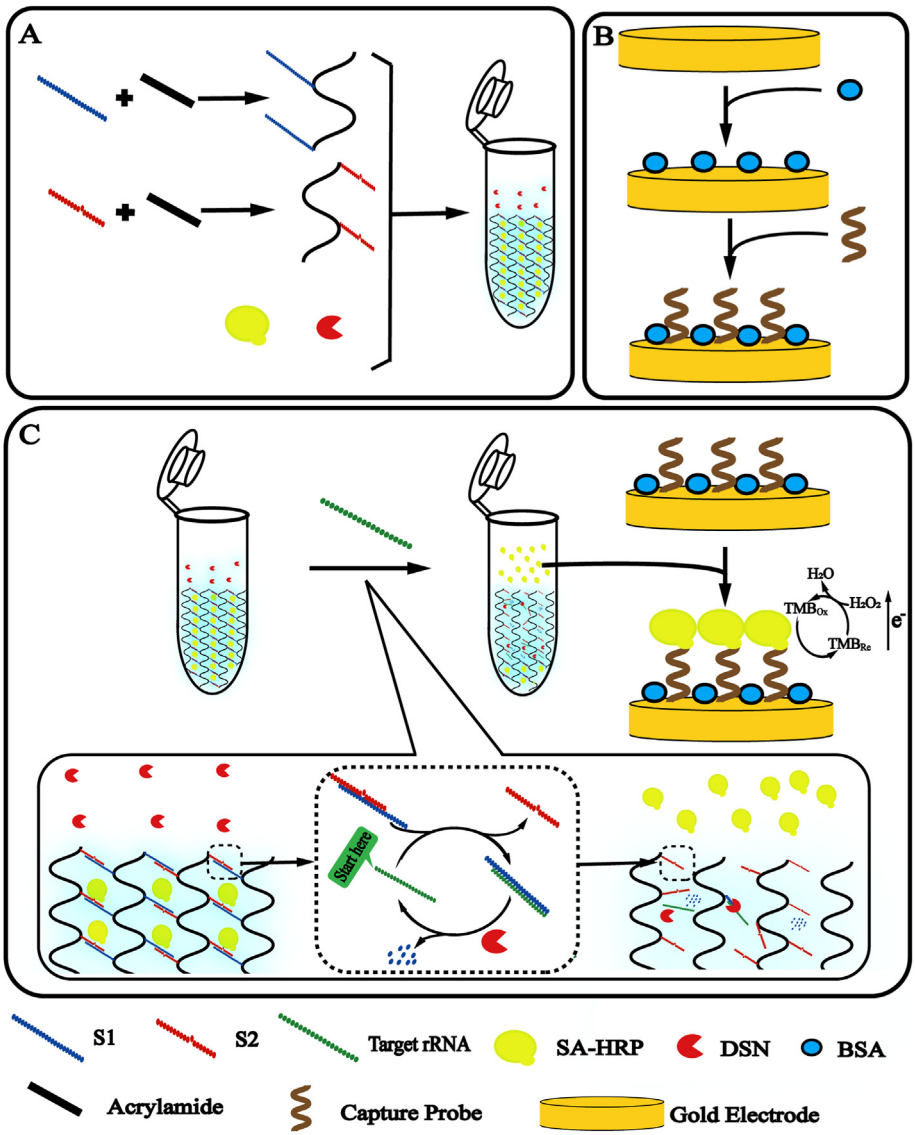

Scheme 1. (A) The diagram of the construction of target-responsive DNA hydrogels. (B) The diagram of the modification process of the bovine serum albumin carrier platform. (C) Schematic illustration of electrochemical biosensor for CT detection based on DSN-assisted target-responsive DNA hydrogels and bovine serum albumin carrier platform.

3.2. Feasibility test

A 20% polyacrylamide gel electrophoresis was used to analyse the target-responsive DNA hydrogel, and the results are shown in Fig. 1A. Lane 3 represents S1-S2 dsDNA, and Lane 4 represents S1-S2 dsDNA with DSN. There was no obvious difference between Lanes 3 and 4, demonstrating that S1-S2 dsDNA and DSN could coexist stably without reaction. Lane 5 represents S1-S2 dsDNA with target rRNA, and Lane 6 represents S1-S2 dsDNA with target rRNA and DSN. Comparing Lanes 3 and 5 shows that the target rRNA would displace S1-S2 dsDNA to the S1-rRNA hybrid duplex by strand replacement reaction. Similarly, comparing Lanes 5 and 6 shows that the brightness of the S1-S2 dsDNA band became darker after adding DSN. These phenomena indicate the following: (1) DSN has no hydrolysis activity on S1-S2 dsDNA without target rRNA; (2) when the target rRNA is present, it has a displacement effect on S1-S2 dsDNA and can cause DSN recognition. (3) The coexistence of target rRNA and DSN can change S1-S2 dsDNA and produce continuous digestion.

Electrochemical impedance spectroscopy was applied to characterize the different modification stages of the working electrode. As shown in Fig. 1B, the impedance of bare gold (curve a) with a small semicircle diameter indicates that the electrons could transfer rapidly on the gold surface. When BSA had been adsorbed onto the electrode surface, the surface impedance (curve b) increased significantly. This is because the protein molecular layer was negatively charged in an electrolyte with a pH of 7.40, which can hinder negatively charged $[Fe(CN)_6]^{3-/4-}$ from reaching the electrode surface for redox reactions. A further increase of impedance was detected after modification with the capture probe (curve c). As many uncovered pores remained between the BSA molecules, the capture probe could be assembled onto the electrode surface through these pores [38]. The capture probe has a negatively charged DNA phosphate backbone that further prevented $[Fe(CN)_6]^{3-/4-}$ from reaching the electrode surface for redox reactions. When SA-HRP reacted with the biotin-modified capture probe, the spatial resistance and charge effect (curve d) increased further.

The SA-HRP captured by the biotin-modified capture probe triggers a typical HRP-based catalytic reaction with TMB and H_2O_2 as substrates, producing a significantly enhanced electrochemical

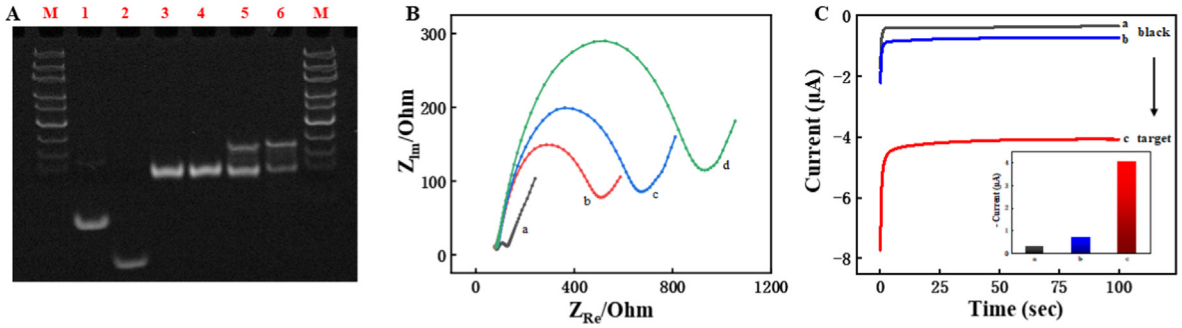

Fig. 1. (A) 20% Polyacrylamide gel electrophoresis analysis of the products. The experimental conditions for lanes 1–6 are described as follows: lane 1) S1; 2) target rRNA; 3) S1-S2 dsDNA; 4) S1-S2 dsDNA + DSN; 5) S1-S2 dsDNA + target rRNA; 6) S1-S2 dsDNA + target rRNA + DSN. (B) The electrochemical impedance measurements of electrodes: a) bare gold; b) BSA/bare gold; c) Probe/BSA/bare gold; d) SA-HRP/Probe/BSA/bare gold. (C) The current signal of the biosensor after hybridization with a) H_2O; b) the supernatant without target rRNA; c) the supernatant with 10 pM of target rRNA. (For interpretation of the references to colour in this figure legend, the reader is referred to the Web version of this article.)

signal. As shown in Fig. 1C, when the blank buffer was dropped on the gold electrode modified with the capture probe, only a small current signal was detected (curve a). When the DNA hydrogel supernatant without the addition of target rRNA was dropped onto the gold electrode modified with capture probes, a very slight increase in the current signal was observed (curve b). This may be due to the nonspecific leakage of SA-HRP, which had been modified on the electrode surface. When the DNA hydrogel supernatant with the target rRNA reaction was dropped onto the gold electrode modified with the capture probe, a significantly enhanced signal was detected (curve c). These phenomena show that (1) the target rRNA can induce the cleavage of the DNA hydrogel and cause the release of SA-HRP; (2) SA-HRP catalyzes the reaction of TMB and H_2O_2, causing a change in the i-t curve.

3.3. Optimization of experimental conditions

Since the modification of the gold electrode surface has a vital influence on the final result of the electrochemical biosensor, the modification of BSA and the capture probe were first optimized. Earlies confirmed that the adsorption time of BSA on the electrode surface is the main factor affecting the subsequent modification, so this time was optimized first [33,34]. Cyclic voltammograms can be used to characterize the adsorption behaviour of proteins on the electrode surface by monitoring the change in potential difference (ΔE) and peak current (ΔIp) between the anode and cathode peaks. As shown in Fig. 2A, as the time for the gold electrode to adsorb BSA increased, ΔIp gradually decreased and ΔE gradually increased. The reason lies in that with the enhanced adsorption time, more BSA adsorbed on the electrode surface, which hindered the electron transfer between ferricyanide and the gold surface. After 15 min, ΔIp and ΔE remained stable, which proved that the monolayer adsorption of BSA on the surface of the gold electrode reached saturation. Therefore, the best adsorption time for BSA was 15 min.

The density of the capture probe on the electrode surface directly affects the adsorption of SA-HRP. As shown in Fig. 2B, the more capture probe used to modify the electrode, a corresponding increase in the current intensity was detected, which reached a plateau after 5 μM. Therefore, 5 μM was chosen in the following study.

S1-S2 dsDNA acts as a cross-linking agent and plays an important role in the formation of DNA hydrogels. The cross-linked hydrogel with a low concentration of S1-S2 dsDNA has higher sensitivity because the hydrogel with less cross-linking agent is easier to disintegrate, but the background signal will be large because of the leakage of SA-HRP. In contrast, too much S1-S2 dsDNA will need more reaction time to destroy the hydrogel. Therefore, the concentration of S1-S2 dsDNA used to prepare the hydrogel was optimized. As shown in Fig. 2C, the signal at present of target (red band) and the background signal (black band) both decreased as the S1-S2 dsDNA concentration increased from 10 μM to 200 μM. The ratio of signal value to background signal (S/B) is used to reconcile the performance requirements of a high target signal with a low background signal. The S/B increased gradually with increasing S1-S2 dsDNA concentrations from 10 μM to 100 μM, but decreased after an inflection point at 100 μM. The largest difference in the current signal appeared at an S1-S2 concentration of 100 μM. Therefore, the optimal concentration of S1-S2 was set to 100 μM.

The SA-HRP enzyme activity unit embedded in the DNA hydrogel was also optimized. The higher enzymatic activity unit of SA-HRP, which is more readily released, results in higher sensitivity of the hydrogel, but at the same time non-specific leakage is increased, resulting in a larger background signal. The S/B value is used to modulate the target and background signals. As shown in Fig. 2D, when the enzymatic activity unit of SA-HRP was raised, both the target and background signals increased. The maximum value of S/B appeared at 0.1 U of the SA-HRP enzyme activity unit. Therefore, the optimal condition of the SA-HRP enzyme activity unit was set to 0.1 U.

Afterwards, the temperature of the DNA hydrogel reaction was optimized, as shown in Fig. 2E. The influence of temperature on the current signal mainly has two aspects: (1) the optimal temperature for DSN is 60 °C, and (2) the melting temperature of the S1-S2 dsDNA is 48 °C. The best temperature should let the enzyme activity of DSN be as high as possible and avoid spontaneous melting of the S1-S2 dsDNA. As shown in Fig. 2E, as the temperature gradually increased from 25 °C to 45 °C, the target current signal (red band) and the background signal (black band) increased. This was because the enzymatic activity of DSN and the spontaneous melting of the S1-S2 dsDNA increased with temperature. While S/B increased between 25 °C and 35 °C, it reached its highest value at 35 °C and then decreased. This result indicated that 35 °C was the optimal reaction temperature for this strategy. At this temperature, the enzyme activity of DSN was still high, but the spontaneous melting of the S1-S2 dsDNA was weak.

Sufficient DSN reaction time and SA-HRP adsorption time on the gold electrode could ensure the release and recapture of large amounts of SA-HRP. Therefore, optimization of the DSN reaction time and SA-HRP adsorption time is important to improve the performance of the biosensor. As shown in Fig. 2F (black part), the current signal increases significantly with time as the DSN response time increases from 30 min to 60 min. And after 60 min, the signal change leveled off, indicating that 60 min was sufficient to

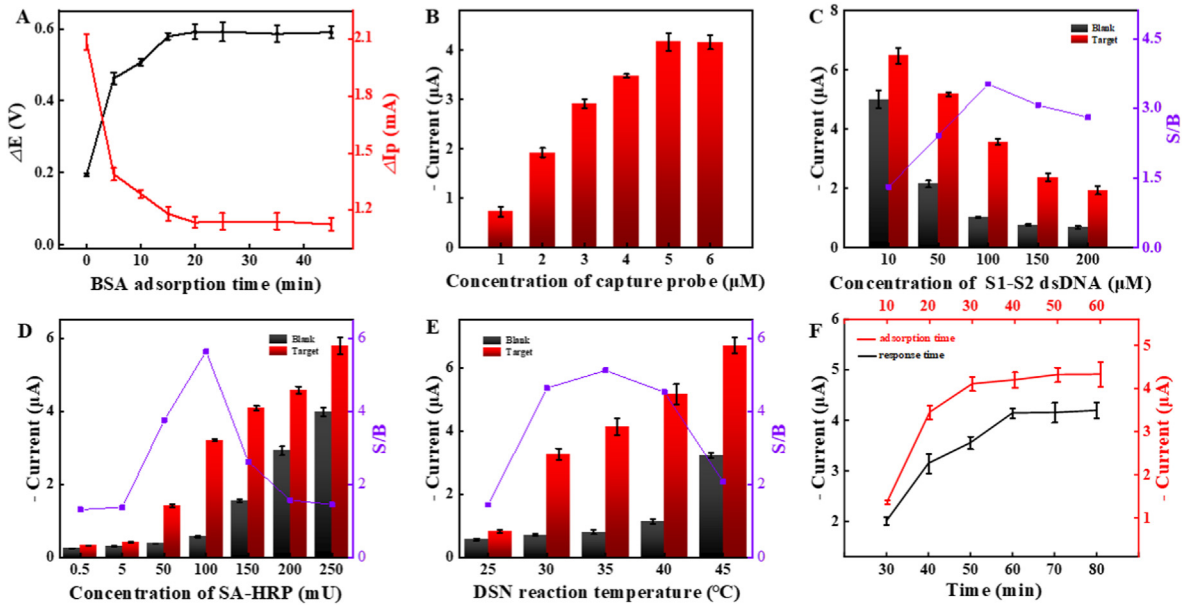

Fig. 2. Effect of (A) the BSA adsorption time; (B) the concentration of capture probe; (C) the concentration of S1-S2 dsDNA; (D) the concentration of SA-HRP; (E) the DSN response temperature; (F) the SA-HRP adsorption time and DSN response time. The concentration of target rRNA was 10 pM. The error bars show the standard deviation of three replicate determinations.

complete the reaction. As shown in Fig. 2F (red part), SA-HRP was adsorbed on the gold electrode from 10 min to 30 min, and the current signal increased rapidly with time. However, after 30 min, the increase in signal value with time slowed down significantly, and a plateau appeared, suggesting that 30 min is sufficient to allow SA-HRP to bind stably to the capture probe. In a short period, the rapid increase in signal value was mainly caused by the efficient and specific binding of SA-HRP with the capture probe. Therefore, 60 min was chosen as the best time for the DSN reaction, and 30 min was chosen as the best time for SA-HRP to be adsorbed on the gold electrode.

3.4. Performance for target rRNA determination

As shown in Fig. 3A, the current intensity increased with increasing target concentration from 0 to 25 pM. A good linear relationship existed between the Δcurrent (current variation with and without the target) and the logarithm of the target rRNA concentration from 10 fM~15 pM. The linear equation could be expressed as follows:

$$\Delta current = 0.951 \times LogC_{rRNA} + 2.211 \cdot R^2 = 0.9970$$

where Δcurrent (unit is μA) is the current intensity of the system and C_{rRNA} (unit is pM) is the concentration of the target. The low detection limit was 5.8 fM by calculating the average signal of the blank plus three times the standard deviation. Because CT infections can lead to many serious diseases and are easily missed, the detection of CT requires a high level of sensitivity for the relevant sensors. Some of the reported CT nucleic acid detection methods (see Table 1) have successfully used sensitive electrochemical detection techniques, but the lack of signal amplification strategies or the mere incorporation of traditional signal amplification strategies such as PCR, results in the inability to further improve sensitivity. Compared with the reported methods for CT nucleic acid detection, the strategy proposed in this work possessed a lower detection limit. The reason for the above phenomenon is that there are two signal amplification processes in the strategy Firstly, the target recovery of the DSN allows a small amount of target rRNA to trigger repeated hydrolysis of the DNA hydrogel, releasing a large amount of SA-HRP and creating the first signal amplification. Secondly, the released SA-HRP catalyzes the redox reaction between TMB and H_2O_2 on the gold electrode surface, which greatly amplifies the current signal and generates an enzymatic amplification. Moreover, the amount of 16S rRNA in CT is much higher than that of DNA, and therefore 16S rRNA is more sensitive as a target for CT detection compared to DNA. The above results indicate that the strategy has a high sensitivity, which has great potential for practical applications in the detection of CT-infected individuals.

The specificity of the electrochemical biosensor was evaluated in response experiments against different rRNA sequences. 16S rRNA fragments included *Neisseria gonorrhoeae* (NG), *Ureaplasma urealyticum* (UU), and *Mycoplasma genitalium* (MG), whose concentrations were much higher (100-fold) than the target rRNA (10 pM) of CT. As shown in Fig. 3B, after adding NG 16S rRNA, UU 16S rRNA, and MG 16S rRNA, the current signal was not changed significantly, while adding CT 16S rRNA caused a strong signal increase. These results indicate the high specificity of the strategy, which may be due to (1) The specificity of DSN plays a powerful role in distinguishing between mismatched sequences. DSN can highly selectively cleave DNA strands in perfectly paired DNA-RNA hybrids, but has no effect on mismatched nucleic acid duplexes [35–37]. (2) The high specificity of base complementary pairing dictates that incompletely matched sequence fragments are difficult to elicit a substitution reaction against the S1-S2 dsDNA strand.

As shown in Fig. 3C, the highly reproducibility of the biosensor was demonstrated by comparison to a method without BSA modification (placing the capture probe directly on the surface of the gold electrode, followed by closure with alkanethiol). The BSA carrier platform decreased the relative standard deviation (RSD) of detecting 10 samples of the same concentration from 8.5% to 4.3% compared to the method without BSA modification. The RSD and the detection limit of the proposed strategy are lower than that of the previously reported microorganism 16S rRNA electrochemical biosensors (as shown in Table 2). The reason for the above

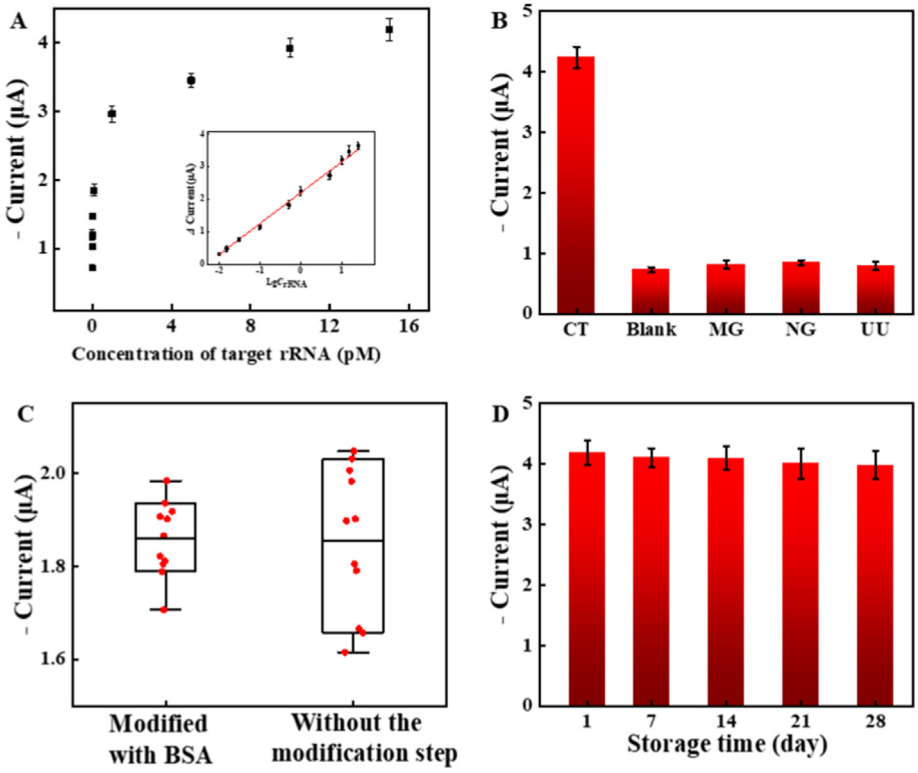

Fig. 3. (A) The relationship between *I-T* current signal and target rRNA sequence concentration. Insert: Calibration curve between the ΔCurrent and the logarithm of the target rRNA sequence concentration. (B) The selectivity of the electrochemical biosensor. [CT] = 10 pM, [MG] = [NG] = [UU] = 1 nM. (C) Measurement of 10 samples of the same concentration with different electrodes. [CT] = 100 fM. (D) The effect of DNA hydrogel storage time. [CT] = 10 pM. The error bars show the standard deviation of three replicate determinations.

Table 1
Comparison of different methods for CT nucleic acid detection.

Target molecule	Detection limit	Time	Detection technology	Reference
DNA	5.9 pM	240 min	Electrochemistry	[40]
DNA	69.5 pM	315 min	Electrochemistry	[13]
DNA	100 nM	180 min	Electrochemistry	[14]
DNA	1.0 nM	The time for PCR + 10 min	PCR + Electrochemistry	[41]
DNA	79.4 fM	280 min	PCR	[42]
DNA	5.0 pM	The time for PCR + 60 min	PCR + DNA microarrays	[43]
DNA	6.7 pM	60 min	Fluorescence	[44]
16S rRNA	5.8 fM	90 min	Electrochemistry	This work

phenomenon is that, when the gold electrode is directly modified by the capture probe, its spatial distribution is relatively random and tends to lie flat on the electrode surface [33,34,39]. In addition, under the nonhomogeneous conditions of the gold electrode surface, the hybridization efficiency of the capture probe to directly capture the target rRNA is unstable [18]. In this work, the BSA-modified electrodes have a porous layer structure with regular gaps to evenly distribute the capture probes, significantly improving the spatial location range and accessibility of the capture probes [38]. At the same time, the DNA hydrogel provides a homogeneous environment for stable recognition of the target sequence and conversion it to easily captured and detected SA-HRP. This results in obtaining a low limit of detection and improving the reproducibility of the biosensor. On the other hand, the storage stability was evaluated by placing the prepared DNA hydrogel in a vacuum box at 4 °C for one month. DNA hydrogel was removed on Days 1, 7, 14, 21 and 28 for the detection of target rRNA (10 pM). The results showed that the DNA hydrogel retained 98.0%, 97.9%, 95.7%, and 95.2% of the initial electrochemical detection signal after storage for 7, 14, 21 and 28 days, respectively, showing the required storage stability of the hydrogel biosensor (Fig. 3D). The reason for the above phenomenon is that DNA hydrogels consist of polyacrylamide and DNA, both of which are structurally simple and stable materials [17], making DNA hydrogels less prone to denaturation and having better storage stability. Based on the above results, the high detection reproducibility and high storage stability of this strategy can provide a stable and reliable result for practical applications of CT detection.

3.5. Application in clinical sample determination

In order to study the practical application of the proposed method, CT 16S rRNA in clinical samples of healthy people and some infected patients had been tested by the developed strategy. As shown in Table 3, electrochemical signals can be detected in clinical samples from the infected patients. And three different concentrations of CT 16S rRNA sequences were added to the clinical samples by standard addition methods. The recovery rate was between 95.1% and 107.7%, and the RSD was between 2.3% and 5.5%. In addition, as shown in Table 4 and 40 clinical samples were collected

Table 2
Comparison of Different Electrochemical Biosensors for Detecting microorganism 16S rRNA[a].

RSD	Detection limit	Linear range	Electrode and modification method	Detection technology	Reference
9.2% (n = 6)	250 pM	250 pM-25 μM	Gold electrode + capture probe + alkanethiol	Cyclic voltammetry	[45]
8.9% (n = 3)	50 CFU/ml (about 6.3 fM)	50 CFU/ml-1.0 × 10^7 CFU/ml (about 6.3 fM-12.6 nM)	Gold electrode + capture probe + alkanethiol	MSPQC method	[15]
6.4% (n = 3)	2.0 pM	2.0 pM−10 pM	Gold electrode + capture probe + alkanethiol	Cyclic voltammetry	[16]
7.4% (n = 6)	2.5 nM	5.0 nM−700 nM	Gold electrode + Mesoporous silica film + capture probe	Cyclic voltammetry	[46]
5.58% (n = 5)	–	0−130 μM	Magnetite on silica + capture probe	Differential pulse voltammetry	[47]
6.8% (n = 3)	0.012 pg/μL (about 1.9 pM)	0.3 pg/ml-600 pg/ml (about 46.5 pM −92.9 nM)	Gold electrode + capture probe	Amperometric detection	[48]
_	10 fM	10 fM-1.0 nM	Gold electrode + capture probe + alkanethiol	Cyclic voltammetry	[49]
_	500 nM	1.9 μM−238 μM	Indium tin oxide electrode	Cyclic voltammetry	[50]
_	10 pM	10 pM-1.0 μM	Indium tin oxide electrode	Cyclic voltammetry	[51]
4.3% (n = 10)	5.8 fM	10 fM-25 pM	Gold electrode + BSA + capture probe	Amperometric detection	This work

[a] Multichannel Series Piezoelectric Quartz Crystal (MSPQC).

Table 3
Detection of targets in clinical samples[a].

Sample	Detected (fM)	Target DNA added (fM)	Total found (fM)	Recovery (%)	RSD (%)
1#	–	10	10.4	97.4	3.5
		100	106.4	106.4	4.4
		1000	1020.8	102.1	3.0
2#	–	10	10.6	106.4	5.2
		100	97.2	97.2	3.5
		1000	1077.3	107.7	4.5
3#	–	10	9.5	95.1	5.5
		100	98.9	98.9	3.8
		1000	1040.7	104.1	2.6
4#	19.0	10	29.0	100.3	2.3
		100	128.1	109.1	4.9
		1000	1070.4	105.1	4.5
5#	193.2	10	202.9	97.1	2.8
		100	290.4	97.3	4.1
		1000	1257.2	106.4	2.5

[a] Sample 1,2 and 3 were from healthy people; sample 4 and 5 were from infected persons.

Table 4
Comparison of test results[a].

The CT nucleic acid detection	This Electrochemical Biosensor		Total
	Positive	Negative	
Positive	19	1	20
Negative	3	17	20
Total	22	18	40

[a] Kappa value = 0.8.

and tested. The Kappa test was used to test the degree of consistency between the results of this method and the results of the CT nucleic acid detection kit, and Kappa value was 0.8. This shows that consistency is excellent. (Kappa value < 0.4 means poor consistency, 0.4 ≤ Kappa value < 0.75 means general consistency, Kappa value ≥ 0.75 means excellent consistency.) These results indicated that the proposed biosensor could be used for CT detection in clinical samples and has a great potential in biological and clinical analyses.

4. Conclusions

A highly reproducible and sensitive electrochemical biosensor has been developed for CT detection, which has several advantages. Firstly, the ordered loading of capture probes by the BSA vector platform combined with the stable signal conversion function of DNA hydrogels, effectively improves the reproducibility of electrochemical assays. Secondly, with abundant CT 16S rRNA fragments as the target and target-responsive DNA hydrogel assisted by DSN as the signal amplification method, incorporating the sensitivity of the electrochemical detection technique, this strategy can achieve ultrasensitive and specific detection of CT. Finally, the method was applied to detect targets in clinical samples with satisfactory results and a good agreement between the proposed method and the classical qualitative method had been reached. This detection strategy has great potential in the clinical pathogen detection and is expected to provide a new method for the extensive screening of genital tract pathogens.

CRediT authorship contribution statement

Lingjun Cheng: Conceptualization, Investigation, Data curation, Writing – original draft. **Yinghao He:** Conceptualization, Investigation, Writing – original draft. **Yuanyuan Yang:** Investigation, Data curation. **Jiaming Chen:** Data curation, Writing – original draft. **Hongzhang He:** Resources. **Yinhuan Liu:** Supervision, Project administration. **Zhenyu Lin:** Supervision, Project administration, Writing – review & editing, Funding acquisition. **Guolin Hong:** Supervision, Project administration, Writing – review & editing, Funding acquisition.

Declaration of competing interest

The authors declare that they have no known competing financial interests or personal relationships that could have appeared to influence the work reported in this paper.

Acknowledgements

This project was financially supported by the National Natural Science Foundation of China (81772287, 81371902) and the Natural Science Foundation of Fujian Province of China (2020J011241).

References

[1] M. Malhotra, S. Sood, A. Mukherjee, S. Muralidhar, M. Bala, Genital Chlamydia trachomatis: an update, Indian J. Med. Res. 138 (2013) 303–316.
[2] G.M. Zhong, R.C. Brunham, L.M. de la Maza, T. Darville, C. Deal, National Institute of Allergy and Infectious Diseases workshop report: "Chlamydia vaccines: the way forward, Vaccine 37 (2019) 7346–7354.
[3] J. Rawre, D. Juyal, B. Dhawan, Molecular typing of Chlamydia trachomatis: an overview, Indian J. Med. Microbiol. 35 (2017) 17–26.
[4] J. Rowley, S. Vander Hoorn, E. Korenromp, N. Low, M. Unemo, L.J. AbuRaddad, R.M. Chico, A. Smolak, L. Newman, S. Gottlieb, S.S. Thwin, N. Broutet, M.M. Taylor, Chlamydia, gonorrhoea, trichomoniasis and syphilis: global prevalence and incidence estimates, Bull. World Health Organ. 97 (2019) (2016) 548–562.
[5] F. Tagini, G. Greub, Chlamydial infections: epidemiology, pathogenesis, diagnosis and treatments, Rev. Med. Suisse 14 (2018) 1620–1625.
[6] E. Lanjouw, S. Ouburg, H.J.D. Vries, A. Stary, M. Unemo, European guideline on the management of Chlamydia trachomatis infections, Nippon. Sanka Fujinka Gakkai Zasshi 37 (2015) (2015) 721–729.
[7] W.E. Stamm, Chlamydia trachomatis - the persistent pathogen - thomas parran award lecture, Sex. Transm. Dis. 28 (2001) 684–689.
[8] A. Ammerdorffer, M. Stojanov, G. Greub, D. Baud, Chlamydia trachomatis and Chlamydia-like bacteria: new enemies of human pregnancies, Curr. Opin. Infect. Dis. 30 (2017) 289–296.
[9] T.T. Kanninen, J. Quist-Nelson, G. Sisti, V. Berghella, Chlamydia trachomatis screening in preterm labor: a systematic review and meta-analysis, Eur. J. Obstet. Gynecol. Reprod. Biol. 240 (2019) 242–247.
[10] S. Shetty, C. Kouskouti, U. Schoen, N. Evangelatos, S. Vishwanath, K. Satyamoorthy, F. ainer, A. rand, Diagnosis of Chlamydia trachomatis genital infections in the era of genomic medicine, Braz. J. Microbiol. 52 (2021) 1327–1339.
[11] J.E. Frew, H.A. Hill, Electrochemical biosensors, Anal. Chem. 39 (2010) 1747–1763.
[12] E. Cesewski, B.N. Johnson, Electrochemical biosensors for pathogen detection, Biosens. Bioelectron. 159 (2020).
[13] S. Baek, J.K. Ahn, B.Y. Won, K.S. Park, H.G. Park, A one-step and label-free, electrochemical DNA detection using metal ion-mediated molecular beacon probe, Electrochem. Commun. 100 (2019) 64–69.
[14] M.L. Sang, S. Shin, H.Y. Kim, B.Y. Won, H.G. Park, Washing-free electrochemical strategy to detect target DNA utilizing peroxidase mimicking DNAzyme, Biotechnol. Bioproc. Eng. 25 (2020) 707–714.
[15] Y. Feng, D. Zhou, L. Gao, F. He, Electrochemical biosensor for rapid detection of bacteria based on facile synthesis of silver wire across electrodes, Biosens. Bioelectron. 168 (2020) 112527.
[16] A. Walter, J. Wu, G.-U. Flechsig, D.A. Haake, J. Wang, Redox cycling amplified electrochemical detection of DNA hybridization: application to pathogen E. coli bacterial RNA, Anal. Chim. Acta 689 (2011) 29–33.
[17] S.M. Schreiner, A.L. Hatch, D.F. Shudy, D.R. Howard, C. Howell, J.L. Zhao, P. Koelsch, M. Zharnikov, D.Y. Petrovykh, A. Opdahl, Impact of DNA-surface interactions on the stability of DNA hybrids, Anal. Chem. 83 (2011) 4288–4295.
[18] A.W. Peterson, R.J. Heaton, R.M. Georgiadis, The effect of surface probe density on DNA hybridization, Nucleic Acids Res. 29 (2001) 5163–5168.
[19] D. Bizzotto, I.J. Burgess, T. Doneux, T. Sagara, H.Z. Yu, Beyond simple cartoons: challenges in characterizing electrochemical biosensor interfaces, ACS Sens. 3 (2018) 5–12.
[20] Y.L. Wen, L.Y. Li, J. Li, M.H. Lin, G. Liu, W. Liang, L. Xu, Y. Li, X.L. Zuo, S.Z. Ren, Y. Zhu, DNA framework-mediated electrochemical biosensing platform for amplification-free MicroRNA analysis, Anal. Chem. 92 (2020) 4498–4503.
[21] J. Lu, J. Wang, X.L. Hu, E. Gyimah, S. Yakubu, K. Wang, X.Y. Wu, Z. Zhang, Electrochemical biosensor based on tetrahedral DNA nanostructures and G-quadruplex-hemin conformation for the ultrasensitive detection of MicroRNA-21 in serum, Anal. Chem. 91 (2019) 7353–7359.
[22] Y.H. He, L.J. Cheng, Y.Y. Yang, P. Chen, B. Qiu, L.H. Guo, Y. Wang, Z.Y. Lin, G.L. Hong, Label-free homogeneous electrochemical biosensor for HPV DNA based on entropy-driven target recycling and hyperbranched rolling circle amplification, Sensor. Actuator. B Chem. 320 (2020).
[23] J. Chen, Y. Zhu, H.J. Liu, L.H. Wang, Tailoring DNA self-assembly to build hydrogels, Top. Curr. Chem. 378 (2020).
[24] R. Liu, Y. Huang, Y. Ma, S. Jia, M. Gao, J. Li, H. Zhang, D. Xu, M. Wu, Y. Chen, Design and synthesis of target-responsive aptamer-cross-linked hydrogel for visual quantitative detection of ochratoxin A, ACS Appl. Mater. Interfaces 7 (2015) 6982–6990.
[25] X. Wang, Y. Sun, Y. Dai, W. Sun, X. Zhu, H. Liu, R. Han, D. Gao, C. Luo, A chemiluminescent biosensor for ultrasensitive detection of adenosine based on target-responsive DNA hydrogel with Au@HKUST-1 encapsulation, Sens. Actuators B-Chem 289 (2019) 56–64.
[26] L. Yan, Z. Zhu, Y. Zou, Y.S. Huang, D.W. Liu, S.S. Jia, D.M. Xu, M. Wu, Y. Zhou, S. Zhou, C.J. Yang, Target-responsive "sweet" hydrogel with glucometer readout for portable and quantitative detection of non-glucose targets, J. Am. Chem. Soc. 135 (10) (2013) 3748–3751.
[27] M.M. Zhao, P.L. Wang, Y.J. Guo, L.X. Wang, F. Luo, B. Qiu, L.H. Guo, X.O. Su, Z.Y. Lin, G.N. Chen, Detection of aflatoxin B-1 in food samples based on target-responsive aptamer-cross-linked hydrogel using a handheld pH meter as readout, Talanta 176 (2018) 34–39.
[28] Y. He, X. Yang, R. Yuan, Y.Q. Chai, Switchable target-responsive 3D DNA hydrogels as a signal amplification strategy combining with SERS technique for ultrasensitive detection of miRNA 155, Anal. Chem. 89 (2017) 8538–8544.
[29] Y.F. Sun, S. Li, R.P. Chen, P. Wu, J. Liang, Ultrasensitive and rapid detection of T-2 toxin using a target-responsive DNA hydrogel, Sensor. Actuator. B Chem. 311 (2020).
[30] S.P. Liu, W.Q. Su, Y.L. Li, L.L. Zhang, X.T. Ding, Manufacturing of an electrochemical biosensing platform based on hybrid DNA hydrogel: taking lung cancer-specific miR-21 as an example, Biosens. Bioelectron. 103 (2018) 1–5.
[31] Y. Liang, X. Jin, F. Yuan, Z. Li, S. Chen, Comparison of rRNA-based and DNA-based nucleic acid amplifications for detection of Chlamydia trachomatis, Neisseria gonorrhoeae, and Ureaplasma urealyticum in urogenital swabs, BMC Infect. Dis. 18 (2018).
[32] J.L. Yang, J. Schachter, J. Moncada, D. Habte, T.M. Lietman, Comparison of an rRNA-based and DNA-based nucleic acid amplification test for the detection of Chlamydia trachomatis in trachoma, Br. J. Ophthalmol. 91 (2007) 293–295.
[33] Y.H. Liu, H.H. Deng, H.N. Li, T.F. Shi, H.P. Peng, A.L. Liu, W. Chen, G.L. Hong, A DNA electrochemical biosensor based on homogeneous hybridization for the determination of Cryptococcus neoformans, J. Electroanal. Chem. 827 (2018) 27–33.
[34] Y.H. He, Y.H. Liu, L.J. Cheng, Y.Y. Yang, B. Qiu, L.H. Guo, Y. Wang, Z.Y. Lin, G.L. Hong, Highly reproducible and sensitive electrochemiluminescence biosensors for HPV detection based on bovine serum albumin carrier platforms and hyperbranched rolling circle amplification, ACS Appl. Mater. Interfaces 13 (2021) 298–305.
[35] A.D. Shagin, A novel method for SNP detection using a new duplex-specific nuclease from crab hepatopancreas, Genome Res. 12 (2003) 1935–1942.
[36] J. Lu, J. Wang, X. Hu, E. Gyimah, S. Yakubu, K. Wang, X. Wu, Z. Zhang, An electrochemical biosensor based on tetrahedral DNA nanostructures and G-quadruplex/hemin conformation for the ultrasensitive detection of microRNA-21 in serum, Anal. Chem. 91 (2019) 7353–7359.
[37] H.Y. Zhu, S.N. Ding, Dual-signal-amplified electrochemiluminescence biosensor for microRNA detection by coupling cyclic enzyme with CdTe QDs aggregate as luminophor, Biosens. Bioelectron. 134 (2019) 109–116.
[38] Y.H. Liu, H.N. Li, W. Chen, A.L. Liu, X.H. Lin, Y.Z. Chen, Bovine serum albumin-based probe carrier platform for electrochemical DNA biosensing, Anal. Chem. 85 (2013) 273–277.
[39] Z.H. Li, B. Zhao, D.F. Wang, Y.L. Wen, G. Liu, H.Q. Dong, S.P. Song, C.H. Fan, DNA nanostructure-based universal microarray platform for high-efficiency multiplex bioanalysis in biofluids, ACS Appl. Mater. Interfaces 6 (2014) 17944–17953.
[40] B.Y. Won, D.W. Lee, S.C. Shin, D.Y. Cho, S.S. Lee, H.C. Yoon, H.G. Park, A DNA intercalation-based electrochemical method for detection of Chlamydia trachomatis utilizing peroxidase-catalyzed signal amplification, Biosens. Bioelectron. 24 (2008) 665–669.
[41] B.Y. Won, S. Shin, R. Fu, S.C. Shin, D.-Y. Cho, H.G. Park, A one-step electrochemical method for DNA detection that utilizes a peroxidase-mimicking DNAzyme amplified through PCR of target DNA, Biosens. Bioelectron. 30 (2011) 73–77.
[42] R. Safarkar, J.F. Mehra Bad I, Z. Noormohammadi, R. Mirnejad, Development a rapid and accurate multiplex real time PCR method for the detection Chlamydia trachomatis and Mycoplasma hominis, J. Clin. Lab. Anal. (2017), e22126.
[43] X. Cao, Y.-F. Wang, C.-F. Zhang, W.-J. Gao, Visual DNA microarrays for simultaneous detection of Ureaplasma urealyticum and Chlamydia trachomatis coupled with multiplex asymmetrical PCR, Biosens. Bioelectron. 22 (2006) 393–398.
[44] C.Y. Lee, H. Jang, H. Kim, Y. Jung, K.S. Park, H.G. Park, Sensitive detection of DNA from Chlamydia trachomatis by using flap endonuclease-assisted amplification and graphene oxide-based fluorescence signaling, Microchim. Acta 186 (2019).
[45] F. Kuralay, S. Campuzano, D.A. Haake, J. Wang, Highly sensitive disposable nucleic acid biosensors for direct bioelectronic detection in raw biological samples, Talanta 85 (3) (2011) 1330–1337.
[46] M. Saadaoui, I. Fernandez, G. Luna, P. Diez, S. Campuzano, N. Raouafi, A. Sanchez, J.M. Pingarron, R. Villalonga, Label-free electrochemical genosensor based on mesoporous silica thin film, Anal. Bioanal. Chem. 408 (2016) 7321–7327.

[47] S. Sheng, L. Liu, Z. Zhao, M. Cai, X. Jiang, Y. Kang, Q. Dai, X. Lu, G. Xie, Electrochemical determination of 16s ribosomal RNA of Mycobacterium tuberculosis using magnetite on silica with DNA-functionalized gold nanoparticles, Anal. Lett. 49 (2016) 1379–1387.
[48] C. Liu, G.M. Zeng, L. Tang, Y. Zhang, Y.-P. Li, Y.-Y. Liu, Z. Li, M.-S. Wu, J. Luo, Electrochemical detection of Pseudomonas aeruginosa 16S rRNA using a biosensor based on immobilized stem-loop structured probe, Enzym. Microb. Technol. 49 (2011) 266–271.
[49] Q. Wang, Y. Wen, Y. Li, W. Liang, W. Li, Y. Li, J. Wu, H. Zhu, K. Zhao, J. Zhang, N. Jia, W. Deng, G. Liu, Ultrasensitive electrochemical biosensor of bacterial 16S rRNA gene based on polyA DNA probes, Anal. Chem. 91 (2019) 9277–9283.
[50] M.M. Khalifa, A.A. Elkhawaga, M.A. Hassan, A.M. Zahran, A.M. Fathalla, W.A. El-Said, O. El-Badawy, Highly specific Electrochemical Sensing of Pseudomonas aeruginosa in patients suffering from corneal ulcers: a comparative study, Sci. Rep. 9 (2019) 18320.
[51] A. Purwidyantri, C.S. Lai, Ieee, Au-Nanoarray by Nanosphere Lithography Sensors for Staphylococcus aureus 16S rRNA, 16th IEEE International Conference on Nanotechnology, IEEE-NANO, 2016, pp. 401–404.